

# Laser-induced fluorescence detection of atmospheric NO<sub>2</sub> with a commercial diode laser and a supersonic expansion

Patricia A. Cleary, Paul J. Wooldridge, and Ronald C. Cohen

Routine observations of atmospheric NO<sub>2</sub> at concentrations ranging from 0.1 to 100 parts per billion are needed for air quality monitoring and for the evaluation of photochemical models. We have designed, constructed, and field tested a relatively inexpensive and specific NO<sub>2</sub> sensor using laser-induced fluorescence. The instrument combines a commercial cw external-cavity tunable diode laser (640 nm) and a continuous supersonic expansion. The total package is completely automated, has a modest size of 0.5 m<sup>3</sup> and 118 kg, and could be manufactured at competitive prices with the current generation of instruments. The sensitivity of the instrument is 145 parts per trillion by volume min<sup>-1</sup> (signal-to-noise ratio of 2), which is more than adequate for monitoring purposes. © 2002 Optical Society of America

OCIS codes: 010.1120, 010.1280, 300.2530, 300.6260.

## 1. Introduction

Accurate, sensitive, and routine measurements of NO<sub>2</sub> are essential to advancing our understanding of the chemistry of air pollution, ozone depletion, and climate change. The U.S. Environmental Protection Agency also explicitly regulates NO<sub>2</sub> mixing ratios, and the states are required to develop plans for monitoring and compliance. Despite numerous calls for true NO<sub>2</sub> measurements,<sup>1</sup> most NO<sub>2</sub> measurements obtained for air monitoring purposes are typically measurements of NO + NO<sub>2</sub> in addition to an unquantifiable fraction of the HNO<sub>3</sub>, alkyl nitrates, peroxy nitrates, and aerosol nitrate present in the atmosphere.<sup>2</sup> Most instruments also lack the sensitivity or knowledge of a zero offset required to accurately monitor daytime concentrations during the summer. Concentrations as low as 1 part per billion by volume (ppbv) are not unusual; measurements to 10% precision at this concentration with a time re-

sponse of faster than 1 min are necessary for quantitative evaluation of photochemical models.<sup>3</sup> Measurements of NO<sub>2</sub> for scientific applications, where frequent attention by highly trained personnel is possible, are usually made by photolysis followed by chemiluminescence.<sup>4,5</sup> Extensive measurements in the remote atmosphere have demonstrated the viability of a two-photon laser induced fluorescence (LIF) approach.<sup>6</sup> There has also been a renewed interest in tunable diode laser absorption spectroscopy technology, for example, Jimenez *et al.* have used a fast-response sensor for cross-road emission measurements.<sup>7</sup>

Recently, several variants of a one-photon LIF approach have been developed.<sup>8–12</sup> Table 1 shows a comparison of current LIF instruments. These systems, except for that developed by Matsumoto *et al.*,<sup>10</sup> all rely on complex laser systems. Fong and Brune used a copper vapor laser-pumped dye laser producing 250 mW at 565 nm to achieve a sensitivity of 460 parts per trillion by volume (pptv) (a signal-to-noise ratio of 2) with 1-min averaging.<sup>8</sup> Thornton *et al.*<sup>11</sup> and Perkins *et al.*<sup>12</sup> used a pulsed YAG-pumped dye laser giving 100–400 mW at 585 nm for excitation. The key factors to achieve high sensitivity with LIF are to produce a near-zero background and maintain high-fluorescence collection efficiency. The Perkins *et al.*<sup>12</sup> experiment was optimized for operation in the lower stratosphere and has a detection limit of approximately 20 pptv min<sup>-1</sup>. Thornton *et al.*<sup>11</sup> worked at lower pressure in the detection cell, from 2

The authors are with the Department of Chemistry, University of California, Berkeley, Berkeley, California 94720. R. C. Cohen (cohen@cchem.berkeley.edu) is also with the Department of Earth and Planetary Science, University of California, Berkeley, Berkeley, California 94720 and the Division of Energy and Environment Technologies, Lawrence Berkeley National Laboratory, Berkeley, California.

Received 9 June 2002; revised manuscript received 27 August 2002.

0003-6935/02/336950-07\$15.00/0

© 2002 Optical Society of America

**Table 1. Operating Conditions and Detection Limits of Contemporary LIF Experiments**

Reference to LIF Variant	Reference	$\lambda$ (nm)	Laser Power (mW)	$\sigma$ ( $10^{-19}$ cm <sup>2</sup> molecule <sup>-1</sup> )	Contrast Ratio (on:off)	LOD <sup>a</sup> (pptv min <sup>-1</sup> )
Fong and Brune (1997)	8	565	250	0.6	2.6:1	460
Perkins <i>et al.</i> (2001)	12	585	100–400	1	3:1	20
Thornton <i>et al.</i> (2000)	11	585	100–400	1	3:1	5
Matsumi <i>et al.</i> (2001)	9	440	100	7	1.8:1	12
Matsumoto <i>et al.</i> (2001)	10	523.5	360	1.4	Not applicable	125
This paper		640.2	16	3.9 <sup>b</sup>	50:1	145

<sup>a</sup>limit of detection given for a signal-to-noise ratio of 2 in 1 min.

<sup>b</sup>Calculated from the Burrows *et al.*<sup>13</sup> room-temperature value of  $1.3 \times 10^{-20}$  cm<sup>2</sup> molecule<sup>-1</sup>  $\times$  30 (enhancement from cooling).

to 4 Torr (1 Torr = 0.1333 kPa) and used a time-delayed gated detection strategy to reduce noise and achieve a sensitivity of 5 pptv min<sup>-1</sup>. Matsumi *et al.*<sup>9</sup> used a 100-mW optical parametric oscillator laser at 440 nm to achieve a detection limit of 12 pptv min<sup>-1</sup>. Giving up the ability to test for interferences, but using a simpler laser system, Matsumoto *et al.*<sup>10</sup> used a Nd:YLF laser harmonic at 523.5 nm to achieve a detection limit of 125 pptv min<sup>-1</sup>.

NO<sub>2</sub> has a continuum absorption that is of comparable intensity to the structured features in its spectrum. The wavelengths chosen by Fong and Brune, Thornton *et al.*, Perkins *et al.*, and Matsumi *et al.* were selected to optimize the product of laser power and the NO<sub>2</sub> cross section, while maintaining the ability to discriminate against interferences by stepping on and off of a spectral feature in the NO<sub>2</sub> spectrum, as demonstrated by the contrast ratio in Table 1. These off-resonance measurements are not used as a measure of the noise, but rather as confirmation that the observed differential fluorescence matches that of the pure molecule, thus indicating that there is no other molecule contributing to the observed fluorescence.

Rapid advances in detector and laser technology are simplifying the optical systems required in these experiments, making LIF extremely promising for routine NO<sub>2</sub> monitoring. Here we describe design and field tests of an LIF instrument for NO<sub>2</sub> detection that uses a simpler, less expensive, commercially available external-cavity tunable diode laser (640 nm). We make up for some of the sensitivity loss that is due to low laser power (16 mW) and small absorption cross section ( $\sigma = 1.3 \times 10^{-20}$  cm<sup>2</sup>/molecule), relative to the instruments described above, by using a continuous supersonic expansion to increase the population in the rotational level excited by the laser. The instrument is smaller and less expensive than any of the LIF instruments that have been previously reported. It is completely automated, extremely reliable, and simple to maintain, making it promising for use by untrained personnel in routine monitoring applications.

## 2. Optical System

Thornton *et al.*<sup>11</sup> describe design criteria for an LIF instrument aimed at detection of ambient NO<sub>2</sub> in detail. The experiment is challenging because of the

small absorption cross section of NO<sub>2</sub>, the rapid quenching of NO<sub>2</sub> fluorescence, and the low concentrations of NO<sub>2</sub> found in the atmosphere. In the instrument described herein, we tried to optimize the sensitivity subject to the design constraint that we utilize a commercially available tunable diode laser. Of the devices on the market at the start of this research, the optimum laser available was determined to be a narrow-linewidth (<1-MHz), single-mode external-cavity tunable diode laser (Tui Optics DL-100) at 640.4 nm (tunable at  $\pm 4.5$  nm), with 16-mW output power. This wavelength range has good overlap with the (080) vibronic band in the X<sup>2</sup>B<sub>2</sub> state of NO<sub>2</sub>.<sup>14</sup> At room temperature, strong rotational features in this band have an absorption cross section of approximately  $1.3 \times 10^{-20}$  cm<sup>2</sup>/molecule.

The laser is focused into a multipass Herriott cell<sup>15</sup> (54 passes), and the fluorescence signal is imaged onto a photomultiplier tube (PMT) (Hamamatsu H7421-50 Select) mounted at 90 deg to the laser beam. The detection cell (Fig. 1) is a vacuum chamber that includes mounts for spherical Herriott cell mirrors at a separation slightly less than twice their radius of curvature (11.6 cm). The laser beam enters the cell through a slit in one mirror, makes 54 passes, and then exits through the same slit. We use mirrors with extremely high reflectivity (Research Electro-Optics, reflectance of 99.998%) because most of the noise in the experiment is due to stray light that results from red-shifted scattering of light that is neither transmitted nor specularly reflected by the mirrors. Also, the polarization of the laser is oriented perpendicular to the detection plane to minimize Rayleigh, Raman, and other scattered laser light. In addition to the high-reflectivity optics, scattered photons that have their source at (or prior to) the mirrors are minimized by a series of baffles that truncate the solid angle of the mirrors as viewed from the center of the cell. The baffles are arranged as a set of concentric rings and disks forming a conical surface in space through which the Herriott beams pass. The disks are mounted directly to the Herriott cell mirrors by a hole drilled in the center of each mirror. The rings are mounted in standard 2-in (5.08-cm) optical tubes (Thorlabs). The baffles are coated with nonfluorescent flat black spray paint (IIT Research Institute formula MH2200).

Fluorescence is collected from the center of the cell

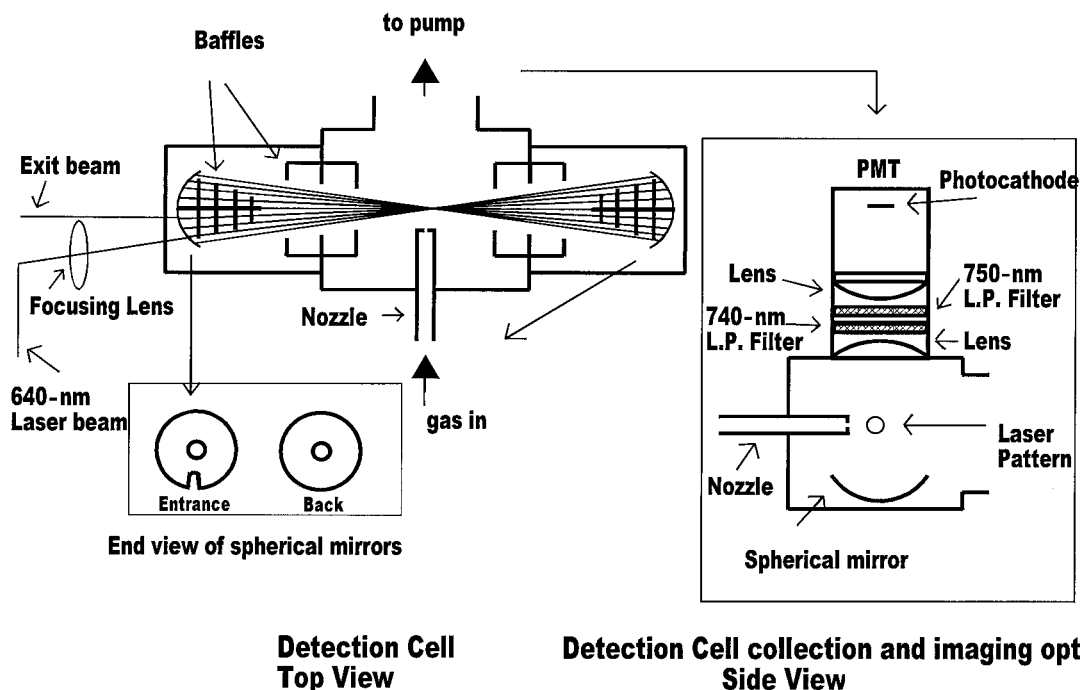


Fig. 1. Detection cell and optics. The laser beam enters through a slit in one of the spherical Herriott cell mirrors (depicted from the front below the cell). It then makes 54 passes, exiting through the same slit. Laser scatter is reduced by two different sets of baffles: (a) solid-disk baffles mounted in the middle of the spherical mirrors and (b) annulus baffles mounted to the walls of the cell. The inlet 1/8-in. (0.32-cm) nozzle with the 350- $\mu$ m-diameter pinhole is held in the cell, close to the edge of the laser beam pattern. The collection optics for the fluorescent photons are shown on the inset to the right, giving a view of the cell perpendicular to the view on the left. A spherical mirror redirects fluorescent photons toward the detector. The photons pass through a collimating lens, a 740-nm long-pass filter (L.P.), a 750-nm long-pass filter, and a focusing lens before striking the PMT.

where the Herriott cell pattern converges to a diameter of 0.6 cm. A 5.08-cm-diameter, 6.5-cm focal-length plano-convex lens mounted 6.5 cm above the center of the cell collects the fluorescence and produces a nearly collimated beam. An aluminum-coated concave mirror (Rolyn Optics) with a 4-cm radius of curvature is mounted 4 cm below the Herriott cell focus (roughly doubling the photon flux aimed at the PMT). The photons then pass through a 740-nm long-pass filter (Omega EFLP740, at least  $10^{-4}$  attenuation at 680 nm), which blocks all the Rayleigh scatter, some of the Raman scatter, and most of the red-shifted laser scatter. This primary filter was built without absorbing components (i.e., colored glass substrates), as these invariably fluoresce, adding noise to what is otherwise a nearly zero background experiment. The 740-nm filter was purchased for the instrument described by Thornton *et al.*<sup>11</sup> In the prototype described here, we follow this filter with a standard commercial 750-nm long-pass filter (CVI). The two filters block the  $O_2$  Raman scattering at 712 nm and most of the  $N_2$  Raman scattering at 754 nm. A fraction of the  $N_2$  scattering leaks through this filter. A filter with a shortwave cutoff of 765 nm, completely eliminating the  $N_2$  Raman, would reduce the noise and lower the detection limit of the instrument. Light that passes through the filters is focused onto the 5-mm-diameter photo-

cathode of the PMT by a 5.08-cm-diameter, 6.5-cm focal-length lens.

The resulting optical system has an approximate geometric collection efficiency of 10% while maintaining a background count rate of 3600 counts  $\text{min}^{-1}$ . Of these, 1560 counts  $\text{min}^{-1}$  are due to the thermal background in the PMT, 550 counts  $\text{min}^{-1}$  are due to Raman scattering of 115 counts (Torr/mW)/min (0.300 Torr; 16 mW), and 1490 counts  $\text{min}^{-1}$  are due to laser scatter.

The laser is kept at constant frequency by use of a peak-finding algorithm and the  $NO_2$  absorption in a reference cell. The 15-cm path-length cell is filled with 30 Torr of pure  $NO_2$ . An uncoated window is used as a beam splitter to pick off 2% of the laser beam. One beam is focused directly on a photodiode, and the less intense beam is directed through the reference cell and then onto a photodiode. The laser diode head is equipped with a piezoactuator controlled externally by an amplified voltage from the computer, which provides fine tuning of the laser frequency. The piezoactuator is used to step the laser on and off the rotational feature of interest every 10 s. Alternate cycles on the peak of the rotational line are shifted by a small fraction ( $\sim 0.5\%$ ) of the peak width. The peak-finding algorithm compares the two signals to identify which is more near the peak of the line and sets the on-line position to match.

This algorithm is capable of keeping up with most laser drifts that do not involve a mode hop or unusually rapid changes in line position.

### 3. Supersonic Expansion

Supersonic expansions are commonly used in the laboratory to produce cold gas phase samples. At low temperatures the population and consequently the absorption cross section of low  $J$  rotational levels increase. Jets are produced when gas is expanded at high pressure into vacuum through a small orifice of either circular or linear geometry. Random motion is converted to forward motion during the expansion—the molecules are moving at high speed in the laboratory frame of reference but at low speeds relative to one another (and consequently low temperatures). The cold region extends to a Mach disk where collisions between the supersonic gas and the background gas in the vacuum chamber produce a shock that rapidly warms the gas to the chamber temperature. The jet temperature that can be achieved is a strong function of the binary collision rate in the nozzle and the expansion ratio, which depend on the backing pressure and nozzle pinhole diameter. The size of the cold region is also a function of these same parameters, where the distance from the nozzle tip to the Mach disk,  $x_m$ , is empirically related to the nozzle pressure  $P_0$ , cell pressure  $P$ , and pinhole diameter  $d$  by the following approximate expression:<sup>16</sup>

$$x_m = d \cdot 0.67 (P_0/P)^{1/2}. \quad (1)$$

The diameter of the Mach disk is roughly  $0.5x_m$ . The rate of two-body collisions slows significantly after the gas has moved a few nozzle diameters from the nozzle.

In our application we seek to produce a jet that is both cold enough to significantly increase the  $\text{NO}_2$  signal and long enough to extend through the 6-mm-diameter laser beam pattern, so we take full advantage of the increased signal. Also, the jet must be long enough that the nozzle can be situated far enough away from the laser beam so as to not cause a dramatic increase in laser scatter. Taken together, these criteria indicate that we target an expansion that is approximately 2 cm long at a rotational temperature below 50 K. We are also subject to the constraint that we are sampling from ambient pressure. We assume that any effort to compress a sample to higher pressure will alter the trace gas composition. A final design criterion is that the expansion should be accomplished by use of pumps that are inexpensive and portable.

Calculations indicate that the achievement of these goals requires a chamber pressure in the neighborhood of 0.2 Torr and gas throughput of the order of 10 Torr  $\text{l s}^{-1}$  such that the aperture diameter is much greater than the mean free path of the ambient gas. For the airborne deployment of our dye-laser-based  $\text{NO}_2$  LIF system,<sup>17</sup> we assembled a lightweight (<45-kg), high-capacity ( $\sim 30\text{-l s}^{-1}$ ) pumping system con-

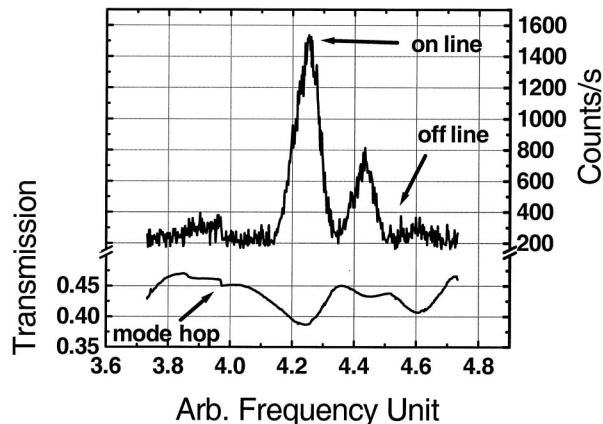


Fig. 2. Fluorescence of 82 ppb of  $\text{NO}_2$  in zero air and corresponding reference cell transmission spectrum of  $\text{NO}_2$  in the region of excitation of  $15,620 \text{ cm}^{-1}$ . The frequencies used for on-line and off-line measurements are indicated with arrows. A diode laser cavity mode hop is also indicated with an arrow.

sisting of a small Roots blower (a commercial automotive supercharger, Eaton Model M-62, 1 l/rev-olution) backed by a  $5.5\text{-l s}^{-1}$  Varian SD-450 mechanical pump, both driven by brushless dc motors (<750 W combined). With these pumps, a continuous expansion of the sample gas through a 350- $\mu\text{m}$ -diameter aperture resulted in a background cell pressure of  $\sim 0.2$  Torr.

Use of the constraints in Eq. (1) predicts a  $\sim 10$ -mm-diameter supersonic expansion that extends to a Mach disk approximately 14 mm downstream of the pinhole. The expected rotational cooling is between 25 and 50 K. Observations of the signal as a function of distance of the nozzle from the laser beam and examination of the relative fluorescence cross sections of several transitions confirm these calculations to be roughly correct.

It would be interesting to produce an even smaller experimental apparatus by a reduction of the pumping requirements. A pulsed supersonic expansion might be effective; however, the decreased duty cycle would result in a lower signal-to-noise ratio unless it was matched to a pulsed laser source. The added complexity would likely increase the need for routine maintenance.

Previous studies<sup>18,19</sup> that used expansions in helium (rather than in air) have found two intense vibronic bands centered at  $15,594$  and  $15,615 \text{ cm}^{-1}$  in jets of a rotational temperature of 4 K. The assignment of these lines is nontrivial and is described in detail by Delon *et al.*<sup>19</sup> Using these experiments as a guide for a search in the warmer jet produced in our experiment, we identified the most intensely fluorescing peak in this spectral region and observed a signal of  $840 \text{ counts min}^{-1} \text{ ppbv}^{-1} \text{ NO}_2$  (Fig. 2). We determined the wavelength to be  $640.17 \text{ nm} \pm 0.2 \text{ nm}$  ( $15,620 \pm 5 \text{ cm}^{-1}$ ) with a 0.5-m monochromator, indicating that we are pumping a line in the vibronic band centered at  $15,615 \text{ cm}^{-1}$  identified by Delon *et al.* Use of the supersonic jet increases the  $\text{NO}_2$  flu-

orescence signal by roughly a factor of 30 over the strongest room-temperature rotational feature available. In addition to the signal increase, the jet reduces the contribution of the nonresonant fluorescence to the background to a negligible quantity, greatly simplifying the process of assessing whether or not there are interferences.

The detection limit of the instrument can be assessed by use of the following signal-to-noise ratio expression, where  $S$  is the signal rate that is due to  $\text{NO}_2$ ,  $B$  is the background, and  $t$  is the collection time. This analysis assumes a shot-noise-limited measurement and that the background is slowly varying and known to arbitrary precision:

$$\frac{S}{N} = \frac{St}{(St + Bt)^{1/2}} \quad (2)$$

Using a signal rate of  $840 \text{ counts min}^{-1}$ ,  $\text{ppb}^{-1}$  (parts per billion), and a background of  $3600 \text{ counts min}^{-1}$ , we calculate a detection limit (signal-to-noise ratio of 2) of  $145 \text{ pptv min}^{-1}$ .

One possible concern associated with use of a supersonic jet for quantitative measurements of  $\text{NO}_2$  is the formation of  $\text{N}_2\text{O}_4$  at low temperatures. At 25 K, at equilibrium, essentially all  $\text{NO}_2$  would be in the form of  $\text{N}_2\text{O}_4$ . We see no evidence for significant  $\text{N}_2\text{O}_4$  formation in the jet and have demonstrated a linear response to  $\text{NO}_2$  at concentrations as high as 100 ppb.

#### 4. Instrument Integration

The optical system along with electronics used to control the laser, vacuum pumps, computer, and all other calibration equipment are mounted within a standard 19-in. (48-cm) instrument rack 150 cm high and 55 cm deep. The lightweight honeycomb-core plate, on which all optics, detection cell, and laser diode are mounted, is placed on 1-in. (2.54-cm) thick rubber pads to dampen vibrations from the pumping system. The instrument weighs 118 kg. The vacuum pumps, which weigh 45 kg, and the optical system, which weighs 23 kg, are the two largest components. The remaining 50 kg are the laser controller, miscellaneous electronics, and the rack itself. The weight and the volume could be trimmed substantially by modest engineering efforts. The power consumption of the instrument is approximately 1.5 kW, half of which is used by the vacuum system. All instrument operations, including sampling, calibrations, and diagnostic tests operate autonomously under the control of software written in LabVIEW (National Instruments).

Long-term stability of the instrument depends on one maintaining a constant temperature at the diode head because changes in the thermal environment of the diode cavity cause mode hops. The thermal system provided by the manufacturer was adequate for experiments in a laboratory setting, where room-temperature fluctuations are slow and minimal. During the course of the field experiments described below, the need for increased thermal stability be-

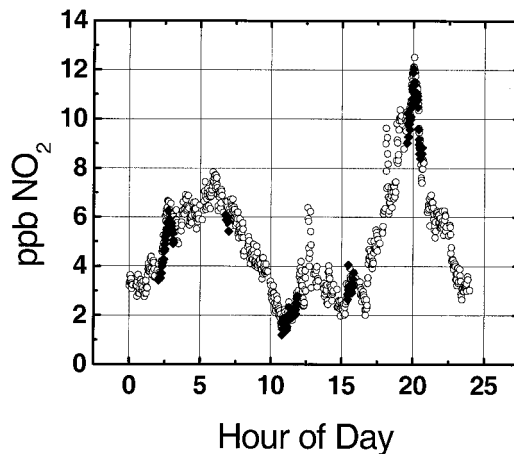


Fig. 3. One-minute averaged  $\text{NO}_2$  measurements made on 3 September 2001 in Granite Bay, California. The open circles represent data from the diode laser LIF instrument, and the solid diamonds represent data taken with the dye-laser LIF instrument.

came clear. The laser worked well within an ambient temperature range in the field station of  $\pm 2 \text{ }^\circ\text{C}$  in the room, which corresponded to  $\pm 0.7 \text{ }^\circ\text{C}$  at the diode head. This was the range observed during the course of the normal diurnal cycling in the field station. The normal fluctuations are slower than  $0.5 \text{ }^\circ\text{C h}^{-1}$ . However, fluctuations outside of that range caused the laser to mode hop. These fluctuations were caused by extended periods of an open trailer door for loading and unloading supplies and by nighttime temperatures that fell well below the air conditioner setpoint, putting the diode housing temperature outside of an acceptable range. To thermally stabilize the laser, a 9.8-W thin-film heater,  $6.5 \text{ cm}^2$  in area, was used to preload the laser temperature controller. The diode head was wrapped with 5-cm-thick small-cell polystyrene foam as primary insulation, and an aluminum cover over the entire optical system served as a secondary thermal boundary and made the system eye safe.

#### 5. Field Evaluation

To evaluate performance of this instrument under realistic operating conditions, a field test and inter-comparison with the 585-nm dye-laser system<sup>11</sup> was conducted at Granite Bay, California, from 18 July to 5 September 2001. Granite Bay, California, is situated midway between Sacramento and the foothills of the Sierra Nevada Mountains. It is in a direct path of the Sacramento plume as it is blown east into the mountains. Example 1-min observations of  $\text{NO}_2$  concentrations on 3 September are shown in Fig. 3. The open circles show observations from the diode laser instrument; the solid diamonds are from the dye-laser instrument. The dye-laser instrument was used to observe  $\text{NO}_2$  for 20-min intervals every 150 min. The rest of the time, the dye-laser instrument was devoted to measurements of  $\text{HNO}_3$ , alkyl nitrates, and peroxy nitrates by thermal dissociation coupled to LIF.<sup>20</sup> The pattern of high and low con-

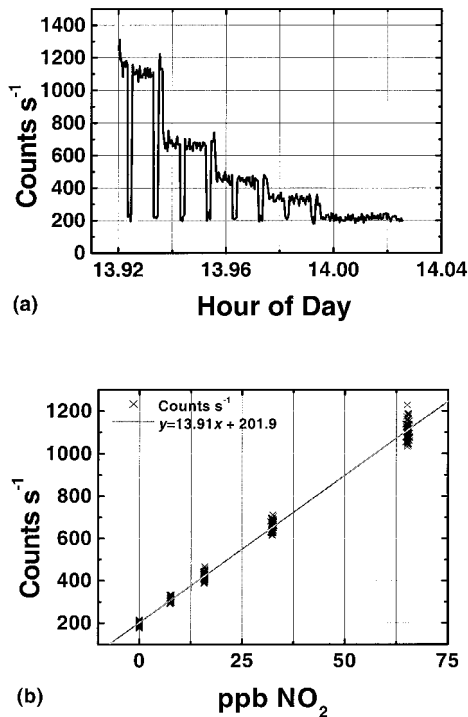


Fig. 4. (a) Calibration on 2 September 2001. Five different mixing ratios of  $\text{NO}_2$  (65.5, 32.5, 15.8, 7.6, and 0 ppb) in zero air are drawn through the sampling tubing. The lack of a slope in the off-line data demonstrates the absence of a  $\text{NO}_2$  continuum fluorescence signal above the noise in the cold  $\text{NO}_2$  spectrum. (b) Data from (a) plotted versus  $\text{NO}_2$  concentration excluding points where the concentration is being changed rapidly to the next step. The slope is 13.91 counts  $\text{s}^{-1}$   $\text{ppb}^{-1}$  (834.6 counts  $\text{min}^{-1}$   $\text{ppb}^{-1}$ ). The noise in the figure is consistent with the shot noise of photon counting.

concentrations shown in Fig. 3 is typical of the observations over the course of the campaign and reflects both the contribution of rush hour traffic and the dynamics of the planetary boundary layer, which is highest during the day and lowest at night.

Both LIF instruments were situated in a temperature-controlled trailer. Inlets for the instruments were mounted adjacent to one another 6 m above the ground on a tower located on the roof of the trailer. The inlets for both instruments drew air from a larger 2-cm-diameter, 10-cm-long tube with a small fan at the back end. Drawing the sampled air in the reverse direction from the normal flow in that tube prevented insects from clogging the inlet. The two instruments were calibrated with the same standard (19.2 parts per million  $\text{NO}_2$  in air, Scott Specialty Gases, Acculife treated cylinder). An automated calibration routine was executed every hour. A typical calibration of the diode laser instrument is shown in Fig. 4. The calibration standard diluted with zero air was added at the inlet on the tower and was drawn through all sampling tubing before entering the cell. Four different mixing ratios were sampled. The calibration constant is determined by a linear fit to these observations of counts versus mixing ratio. Over the course of the

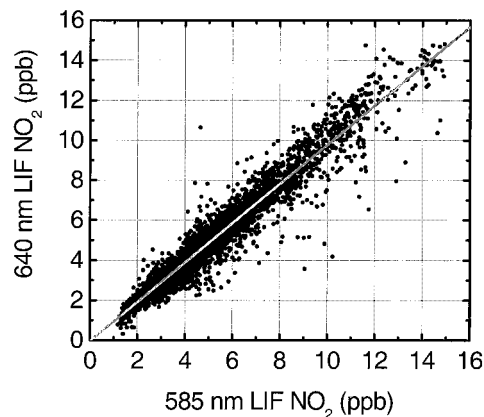


Fig. 5. Intercomparison of 1-min averaged  $\text{NO}_2$  data from Granite Bay with the tunable diode laser instrument at 640 nm and the dye-laser instrument at 585 nm. Slope is 0.975,  $R^2 = 0.927$  with 3735 data points. Omitted are data with plumes on time scales of less than 1 min, because instrument clocks were not synchronized precisely enough to ensure averaging over the same time interval.

campaign, the average calibration constant decreased from 17 counts  $\text{s}^{-1}$   $\text{ppb}^{-1}$  to 14 counts  $\text{s}^{-1}$   $\text{ppb}^{-1}$  (1020–840 counts  $\text{min}^{-1}$   $\text{ppb}^{-1}$ ). This change is attributable to a decrease in laser power from the aging of the diode laser. Consecutive calibrations varied by  $\pm 5\%$  as a result of alignment and power variations caused by temperature fluctuations at the field station. The noise in Fig. 4(b) is consistent with the shot noise of photon counting. At the time of the Granite Bay experiments, the instrument had a relatively high background count rate (12,000 counts  $\text{min}^{-1}$ ) because of excessive laser scatter off of the nozzle. We achieved lower background levels (3600 counts  $\text{min}^{-1}$ ) after the campaign by reblackening the nozzle tip.

Comparison of the  $\text{NO}_2$  measurements made with these two instruments are shown in Fig. 5. The slope of the linear fit (640-nm diode laser  $\text{NO}_2 = m \times 585\text{-nm dye-laser } \text{NO}_2$ )  $m$  is 0.975 with  $R^2 = 0.927$ . The data shown include all measurements from 18 July to 4 September 2001 with the exception of data that were not collected within 2 h of a calibration, or that represent plumes where the  $\text{NO}_2$  concentration was varying faster than 1  $\text{ppb min}^{-1}$ . Both instruments are capable of responding on these rapid time scales, but we did not make the effort to precisely synchronize the instrument clocks, making the comparison difficult. In addition, the data from the diode laser instrument were filtered of spurious data generated during times of laser frequency instability. These instabilities were thermally driven and were recognized by the changes in the absorbance through the  $\text{NO}_2$  reference cell. The relative absorption ( $I/I_0$ ) at the on-line position was an indication of the correct laser frequency. Improvements to laser thermal stability lead to an increase in the amount of reliable data. By the end of the field campaign, a thermal design capable of preventing laser mode hops through most routine events was achieved.

## 6. Conclusion

We have described a LIF instrument utilizing a 640-nm tunable diode laser in conjunction with a supersonic jet for detection of  $\text{NO}_2$  *in situ* with a sensitivity of  $145 \text{ pptv min}^{-1}$ . The instrument is lightweight (118 kg), compact ( $0.5 \text{ m}^3$ ), and has operated autonomously for up to 15 days. Comparison with our more established 585-nm dye-laser LIF instrument shows that the instruments agree to within the precision of the measurements and calibration system.

The sensitivity of this instrument is already adequate for many monitoring applications, and higher sensitivity can be gained by use of lasers with higher power or at wavelengths with larger  $\text{NO}_2$  absorption cross sections (particularly in the 400–450-nm region) when robust versions become available. Better stray-light baffling in the fluorescence cell and fluorescence filters that cut out all Raman-scattered wavelengths will also lower the detection limits. Also, higher pumping capacity would result in higher signal rates (through colder jet temperatures) and would enable reductions in the background scattering (the jet would be longer in extent, so the nozzle tip could be pulled further back from the laser pattern), but at the expense of increased power consumption and weight.

This research was supported by the NASA Instrument Incubator Program under contract NAS1-99053, the National Science Foundation Atmospheric Chemistry Program under grant ATM-0138669, and the U.S. Department of Energy under contract DE-AC03-76SF0009.

## References

1. G. S. Tonnesen and R. L. Dennis, "Analysis of radical propagation efficiency to assess ozone sensitivity to hydrocarbons and  $\text{NO}_x$ . 1. Local indicators of instantaneous odd oxygen production sensitivity," *J. Geophys. Res.* **105**, 9213–9225 (2000).
2. W. A. McClenny, E. J. Williams, R. C. Cohen, and J. Stutz, "Preparing to measure the effects of the  $\text{NO}_x$  SIP call—methods for ambient air monitoring of  $\text{NO}$ ,  $\text{NO}_2$ ,  $\text{NO}_y$  and individual  $\text{NO}_z$  species," *J. Air. Waste Manage.* **52**, 542–562 (2002).
3. J. A. Thornton, P. J. Wooldridge, R. C. Cohen, M. Martinez, H. Harder, W. H. Brune, E. J. Williams, J. M. Roberts, F. C. Fehsenfeld, S. R. Hall, R. E. Shetter, B. P. Wert, and A. Fried, "Ozone production rates as a function of  $\text{NO}_x$  abundances and  $\text{HO}_x$  production rates in the Nashville urban plume," *J. Geophys. Res.* **107**, 10.1029/2001JD000932 (2002).
4. T. B. Ryerson, E. J. Williams, and F. C. Fehsenfeld, "An efficient photolysis system for fast-response  $\text{NO}_2$  measurements," *J. Geophys. Res.* **105**, 26447–26461 (2000).
5. R. S. Gao, E. R. Keim, E. L. Woodbridge, S. J. Ciciora, M. H. Proffitt, T. L. Thompson, R. J. McLaughlin, and D. W. Fahey, "New photolysis system for  $\text{NO}_2$  measurements in the lower stratosphere," *J. Geophys. Res.* **99**, 20673–20681 (1994).
6. J. Bradshaw, D. Davis, J. Crawford, G. Chen, R. Shetter, M. Muller, G. Gregory, G. Sachse, D. Blake, B. Heikes, H. Singh, J. Mastromarino, and S. Sandholm, "Photofragmentation two-photon laser-induced fluorescence detection of  $\text{NO}_2$  and  $\text{NO}$ : comparison of measurements with model results based on airborne observations during PEM-Tropics A," *Geophys. Res. Lett.* **26**, 471–474 (1999).
7. J. L. Jimenez, G. J. McRae, D. D. Nelson, M. S. Zahniser, and C. E. Kolb, "Remote sensing of  $\text{NO}$  and  $\text{NO}_2$  emissions from heavy-duty diesel trucks using tunable diode lasers," *Environ. Sci. Technol.* **34**, 2380–2387 (2000).
8. C. Fong and W. H. Brune, "A laser induced fluorescence instrument for measuring tropospheric  $\text{NO}_2$ ," *Rev. Sci. Instrum.* **68**, 4253–4262 (1997).
9. Y. Matsumi, S. Murakami, M. Kono, K. Takahashi, M. Koike, and Y. Kondo, "High-sensitivity instrument for measuring atmospheric  $\text{NO}_2$ ," *Anal. Chem.* **73**, 5485–5493 (2001).
10. J. Matsumoto, J. Hirokawa, H. Akimoto, and Y. Kajii, "Direct measurement of  $\text{NO}_2$  in the marine atmosphere by laser-induced fluorescence technique," *Atmos. Environ.* **35**, 2803–2814 (2001).
11. J. A. Thornton, P. J. Wooldridge, and R. C. Cohen, "Atmospheric  $\text{NO}_2$ : *in situ* laser-induced fluorescence detection at parts per trillion mixing ratios," *Anal. Chem.* **72**, 528–539 (2000).
12. K. K. Perkins, T. F. Hanisco, R. C. Cohen, L. C. Koch, R. M. Stimpfle, P. B. Voss, G. P. Bonne, E. J. Lanzendorf, J. G. Anderson, P. O. Wennberg, R. S. Gao, L. A. Del Negro, R. J. Salawitch, C. T. McElroy, E. J. Hintsa, M. Loewenstein, and T. P. Bui, "The  $\text{NO}_x$ - $\text{HNO}_3$  system in the lower stratosphere: insights from *in situ* measurements and implications of the  $\text{J}(\text{HNO}_3)$ - $[\text{OH}]$  relationship," *J. Phys. Chem. A* **105**, 1521–1534 (2001).
13. J. P. Burrows, A. Dehn, B. Deters, S. Himmelmann, A. Richter, S. Voigt, and J. Orphal, "Atmospheric remote-sensing reference data from GOME: Part I. Temperature-dependent absorption cross-sections of  $\text{NO}_2$  in the 231–794 nm range," *J. Quant. Spectros. Radiat. Transfer* **60**, 1025–1031 (1998).
14. J. C. D. Brand, K. J. Cross, and A. R. Hoy, "Resonance fluorescence intensities and vibrational assignments in the  $\text{A}^2\text{B}_2$  state of  $\text{NO}_2$ ," *Can. J. Phys.* **60**, 1081–1087 (1982).
15. D. Herriott, R. Kompfner, and H. Kogelnik, "Off-axis paths in spherical mirror interferometers," *Appl. Opt.* **3**, 523–526 (1964).
16. D. R. Miller, "Free jet sources," in *Atomic and Molecular Beam Methods*, G. Scoles, ed. (Oxford U. Press, New York, 1988), pp. 14–53.
17. J. A. Thornton, "Nitrogen dioxide, peroxy nitrates and the chemistry of tropospheric ozone production: new insights from *in situ* measurements," Ph.D. dissertation (University of California, Berkeley, Berkeley, Calif., (2002).
18. R. E. Smalley, L. Wharton, and D. H. Levy, "Fluorescence excitation spectrum of rotationally cooled  $\text{NO}_2$ ," *J. Chem. Phys.* **63**, 4977–4989 (1975).
19. A. Delon, R. Jost, and M. Jacon, "Laser induced dispersed fluorescence spectroscopy of 107 vibronic levels of  $\text{NO}_2$  ranging from 12000 to  $17600 \text{ cm}^{-1}$ ," *J. Chem. Phys.* **114**, 331–344 (2001).
20. D. A. Day, P. J. Wooldridge, M. B. Dillon, J. A. Thornton, and R. C. Cohen, "A thermal dissociation laser-induced fluorescence instrument for *in situ* detection of  $\text{NO}_2$ , peroxy nitrates, alkyl nitrates, and  $\text{HNO}_3$ ," *J. Geophys. Res.* **107**, 10.129/2001JD000779 (2002).